

THREE DIMENSIONAL FINITE ELEMENT ANALYSIS OF FLEXIBLE PAVEMENTS  
TO ASSESS THE EFFECTS OF WANDER AND WHEEL CONFIGURATION

By:

Dona Johnson, Beena Sukumaran, Yusuf Mehta, and Mike Willis  
Civil and Environmental Engineering, Rowan University  
201 Mullica Hill Rd  
Glassboro, NJ 08028  
USA

Phone: (856) 256-5324; Fax: (856) 256-5242

[dona.johnson@navy.mil](mailto:dona.johnson@navy.mil)

[sukumaran@rowan.edu](mailto:sukumaran@rowan.edu)

[mehta@rowan.edu](mailto:mehta@rowan.edu)

[willis84@students.rowan.edu](mailto:willis84@students.rowan.edu)

PRESENTED FOR THE  
2007 FAA WORLDWIDE AIRPORT TECHNOLOGY TRANSFER CONFERENCE  
Atlantic City, New Jersey, USA

April 2007

## ABSTRACT

Current design methods for airfield pavements are becoming inadequate due to the introduction of larger and heavier aircraft with more complex wheel configurations. The purpose of this study is to measure and assess the effects of wander of various wheel configurations on the mechanical response of the pavement layers using three-dimensional finite element analysis. Computationally intensive three-dimensional models are necessary because two-dimensional models cannot sufficiently capture the stress interactions between separate tires of a triple-dual-tandem (TDT) axle used on B-777 and A-380 aircrafts. This study focuses on modeling both medium and low strength subgrade in flexible pavements. Elasto-plastic model is used to simulate the stress-strain response of the base, subbase, and subgrade layers and viscoelastic material properties to model the asphalt layer. The available failure data from the National Airport Pavement Test Facility (NAPTF) [1] of the Federal Aviation Administration based in Atlantic City is used to calibrate the finite element models. The results of this study show that the layers that make up airport pavements can be modeled using a combination of viscoelastic and elasto-plastic properties. The data collected from this study will show the effects of wander on flexible airport pavements. Also studied are correlations between deformations from a single wheel and a 4- and 6- gear configuration. This study is the first critical step in quantifying the damage due to wheel configuration and wander. This will provide an invaluable tool in future design of airfield pavements.

## INTRODUCTION

Three-dimensional finite element analysis tools are increasingly viewed as the best approach to answering certain fundamental questions about pavement performance [2, 3, 4], but the tedious processing and time required to accurately model pavement systems have hampered the use of these analyses. While two-dimensional axi-symmetric models can be utilized for a single wheel load analysis, such a constraint would lead to an inaccurate three-dimensional analysis, particularly for pavements subjected to multiple wheel loads and wander.

As stresses and strains are increasingly used to predict pavement distresses, and thus the relative condition of the various layers in the pavement structure, the need for consideration of non-linear material behavior becomes increasingly important. Linear elastic approximations of unbound material behavior are no longer acceptable in pavement analysis. The stress state dependency of granular materials, and strain based subgrade soil models must be considered for an accurate estimation of true pavement response [5].

Past flexible pavement models used multi-layer elastic analysis, which assumes static loading, whereas in reality pavements are subjected to both static and moving loads. The model used in the study conducted by Zaghoul and White [6] incorporated an elasto-plastic model for the base, sub-base and subgrade and a viscoelastic model for the asphalt layer. Zaghoul and White [6] researched the ability of three-dimensional dynamic finite element programs to predict the response of moving loads on pavement structures. The validation of their model was accomplished by testing the model's ability to predict deformations under static and dynamic load conditions. The final results showed that their model was capable of simulating truckloads and realistic deformation predictions were obtained.

The purpose of this study is to evaluate the effects of wander and wheel configurations on flexible airport pavement. This study includes development of three-dimensional finite element

models, which can reasonably predict pavement performance under aircraft loading. Development of these models requires suitable choice of material properties, which can be validated using actual test data. For this study, full scale testing data, field test data and laboratory test data from the NAPTF were used for validation of the selected material properties. The paper will describe briefly the material property selection process as well as results from simulations to compare wheel configuration in static loading and quasi-static loading with wander.

Several assumptions were made in order to use finite element models. First, data gathered from FAA tests assumes that test sections were properly constructed with perfect mixes in each layer. It is possible that there are other variables that would affect the data that were assumed to be negligible for these models. The finite element models assume that each layer is perfectly bonded so that there is no friction between layers.

## **MATERIAL VERIFICATIONS**

### **Introduction**

Material properties used in the Finite Element Model are critical to the accuracy of the model performance and behavior. Considerable effort during this study was spent on material verification and determination of suitable material models and properties for the various pavement materials that comprise the pavement system. The California Bearing Ratio (CBR) test was used to calibrate the model's material properties for the subbase, base and subgrade. The subgrade was tested to determine the elastic modulus that accurately depicts the real materials response to stress. The subbase and base have an assumed elastic modulus and the CBR test is used to find the corresponding friction and dilation angles. Viscoelastic and Drucker Prager material properties of the asphalt layer were calibrated with the results of the CBR tests. These simulations were used to identify the correct instantaneous elastic modulus and shift factor needed to allow the results to fit full-scale test data for viscoelasticity. They are also used to find the plasticity model parameters, which are a combination of elastic modulus, friction and dilation angle, and cohesion that will best fit the FAA Static Punch Test conducted March 2001 [1]. These verification studies will be further described in this section.

### **California Bearing Ratio Model**

The purpose of using California Bearing Ratio (CBR) test data is to determine the friction angle and dilation angle that will correspond to the given elastic modulus for each pavement material including the base, subbase and subgrade. Once the program is run, the amount of stress on the material after 0.1-inch penetration is determined and compared against a reference material, the percentage of which is then compared against material data sheets provided by the FAA.

The finite element mesh used for the analysis was 10 inches [25.4cm] by 10 inches [25.4cm] and is shown below. A three-dimensional response is simulated using quasi three-dimensional Fourier analysis elements (CAXA8R) available within ABAQUS [7]. CAXA elements are biquadratic, Fourier quadrilateral elements. The number of elements and nodes in the mesh are 185 and 6260 respectively. CAXA elements were used because of their ability to accurately predict the response of axially symmetric loaded models.

The center of the mesh was defined to displace 0.2 inches, thereby acting like the penetration of a piston into a soil sample. Sukumaran et al. [8] found that using the stress-strain data from the

resilient modulus tests from the NAPTF in the material model resulted in the best approximation of the material response for the medium strength Dupont clay. This study will do the same for the low strength Dupont clay, P-154 subbase and P-209 base materials.

Several studies were conducted to validate the material properties for each material type. The material properties used were from the NAPTF laboratory testing. The material properties input into the finite element model during the validation studies are shown in Table 1.

Table 1.  
Material Properties for Material Verification.

Material Property	Material			
	P-154	P-209	Dupont (Low)	Dupont (Medium)
Modulus, psi (MN/m <sup>2</sup> )	20,000 (137.9)	40,000 (275.8)	3,000 (20.68)	11,000 (75.84)
Poisson's Ratio	0.35	0.3	0.45	0.45
Friction Angle	35,40,45,50	32,40,44,48,52	0	0
Dilation Angle	0,5,10	0,5,10	0	0
Cohesion, psi (kN/m <sup>2</sup> )	6.4 (44.1)	5 (34.5)	**	**
Density, pcf (kg/m <sup>3</sup> )	151 (2420)	161 (2580)	95 (1520)	95 (1520)

\*\* Stress-strain values were entered into input files.

The first material tested was the medium strength Dupont clay. The results of the analysis were compared with the raw CBR data from the NAPTF. Figure 1 displays the results of the analysis from Sukumaran et al. [8].

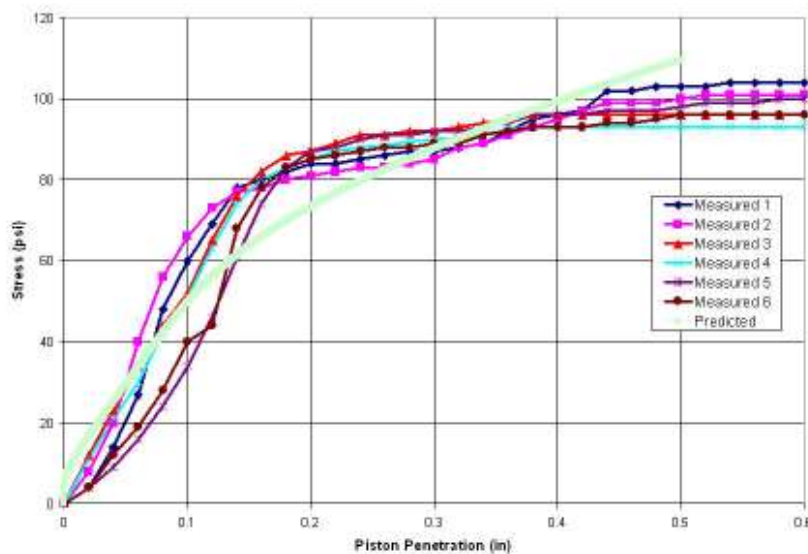


Figure 1. Stress vs. Displacement Plot for Six Field Tests and FEM Prediction from Medium Strength Dupont Clay.

The model was able to capture a fairly accurate response as compared to the measured values; this plot is presented only for completeness and will not be discussed in later sections. The low strength Dupont clay was analyzed in a similar manner, with the raw CBR data from the NAPTF and the predicted data from finite element modeling. The final results of the validation study are listed in table 8 shown later in the paper.

Stress-strain data was not available for P-154 and P-209 and so the results from the model were compared directly with the CBR values. It is a two step process to determine the appropriate friction and dilation angle for each material. First a series of input files were created with different friction angles in the expected range as obtained from laboratory tests conducted by the NAPTF with dilation angles of zero. The total amount of stress over the surface of the piston affected area was summed up and compared against a baseline material summed stress, which gives a CBR value. Comparing this value against the target CBR value, or average CBR value from lab testing, gives the friction angle that corresponds to the elastic modulus chosen for this material. Below is the output from testing the friction angles of the base material P-209.

Table 2.  
Predicted CBR Values for P-209.

Friction Angle, degrees	CBR at Displacement of 0.1 in.
32	11.78
40	18.16
44	23.97
48	33.69
52	51.44
Target CBR	44

From this chart, the friction angle was concluded to range between 48 and 52°, and therefore was assumed to be an average of 50° for use in the finite element models. The next set of input files fix the friction angle at 50°, while altering dilation angles to determine the value that would give a CBR value close to that of the average value taken from the material data from the FAA [1].

From the various validation studies, the P-209 base was assumed to have a friction angle of 50 degrees, and a dilation angle of 5 degrees. This process was repeated for the subbase (P-154) layer.

The final properties used for the various materials used in the pavement system are shown below in Table 3. More details of the validation studies are provided in Willis [9]. The results from the CBR modeling showed that the material properties being used were able to accurately capture the response of the material when subjected to the CBR test.

## ASPHALT SURFACE LAYER VERIFICATION STUDIES

### Static Punch Test

The FAA had conducted a test called the Static Punch test [1]. Within this test a trench was cut out of a medium strength subgrade flexible pavement section (MFC), and a 6-wheel B-777 landing gear configuration spacing was used. The landing gear's first set of wheels was placed approximately 20 inches away from the edge of the trench. The loading was gradually increased from zero to around 55 kips per wheel, and allowed to remain at this load for the remainder of the test. Afterwards the deformation and force were recorded. The results of this test helped to

verify the material properties ascertained through other FEM model verification studies and also helped to determine the accuracy of the whole pavement system. The goal of any model in finite element analysis is to have similar results to full-scale test data.

Table 3.

Properties of the Various Materials Comprising the Pavement System Obtained from Validation Studies.

Material Property	Material			
	P-154	P-209	Dupont (Low)	Dupont (Medium)
Modulus, psi (MN/m <sup>2</sup> )	20,000 (137.9)	40,000 (275.8)	3,000 (20.68)	11,000 (75.84)
Poisson's Ratio	0.35	0.3	0.45	0.45
Friction Angle	45	50	0	0
Dilation Angle	5	5	0	0
Cohesion, psi (kN/m <sup>2</sup> )	6.4 (44.1)	5 (34.5)	**	**
Density, pcf (kg/m <sup>3</sup> )	151 (2420)	161 (2580)	95 (1520)	95 (1520)



Figure 2. Static Punch Test on MFC Pavement 3/01.

### Viscoelasticity Model

In order to describe the viscoelastic properties of asphalt, a Prony series expression is used. A Prony series consists of  $n$ -pairs of parallel spring dashpot assemblies. Equation (1) describes such a series [10].

$$E(\xi) = \sum_{i=1}^n E_i e^{-\xi/\lambda_i} \quad (1)$$

where:  $E(\xi)$  = relaxation modulus at reduced time  $\xi$

$E_i$  = spring constants or modulus

$\lambda_i$  = relaxation time

Equation (1) only describes the elastic modulus at a specific temperature also known as a reference temperature. To determine the relaxation moduli at other temperatures, a principle of time-temperature superposition is used. This principle replaces real time which corresponds to the temperature of interest, with reduced time which is related to the reference temperature. Equation (2) describes this principle.

$$\xi = \frac{t}{a_t} \quad (2)$$

where:  $\xi$  = reduced time

$t$  = real time

$a_t$  = temperature shift factor

Table 4 below, from Bozkurt and Buttlar [10], shows the starting point for this model. The data describes a prony series model for a different formulation of asphalt than that used in airfield pavements. However, the relationship between relaxation times and the relationship between elastic moduli are constant for most asphalt materials, so the numbers below were used as the basis for this verification study.

Table 4.

Initial Prony Series to describe Elastic Modulus of Asphalt Concrete [1].

Prony Series Parameters for PG 58-22 Overlay Mix				
Spring Constants, ksi (N/m <sup>2</sup> x 10 <sup>6</sup> )				
$E_1$	$E_2$	$E_3$	$E_4$	$E_5$
5502 (798)	1489 (216)	5143 (746)	5565 (807)	6594 (956)
Relaxation Times, sec				
$\lambda_1$	$\lambda_2$	$\lambda_3$	$\lambda_4$	$\lambda_5$
8.1	101	826	6560	176087

### Viscoelasticity Model

The next FE model was used to identify the instantaneous total elastic modulus as well as the shift factor required for the relaxation times to match the static punch test data from underneath the furthest wheel away from the trench. This wheel was chosen because it would have the least influence from the boundary conditions of the trench. It would almost act as if there was no trench at all.

The dimensions of the model are 12 feet (3.66 m) wide by 21 feet (6.4 m) long by 6 feet (1.83m) deep, with a layer of infinite elements on the last 6 inches (15 cm) of pavement. The cross section matches that of a standard medium strength flexible pavement with conventional

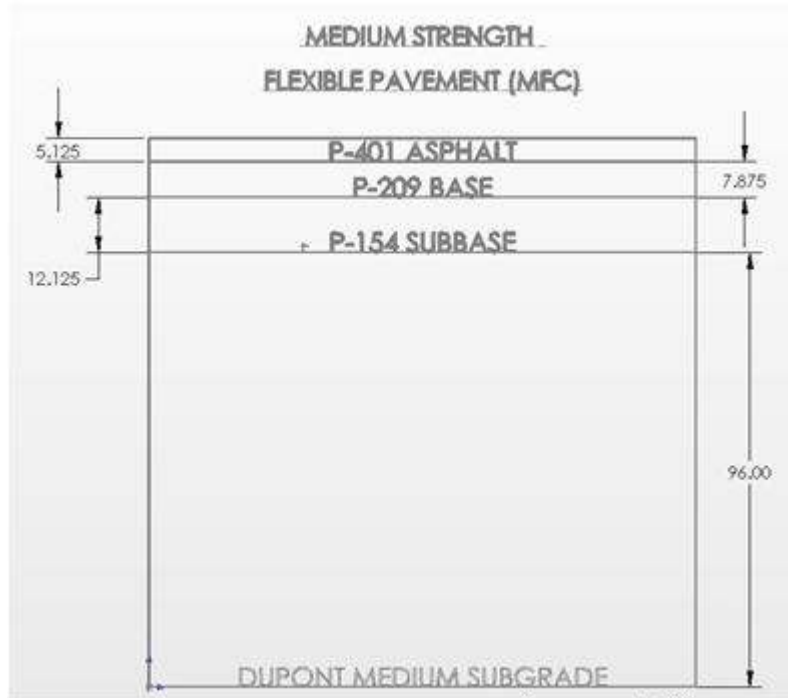


Figure 3. MFC Pavement Cross Section (dimensions in inches).

base (MFC), which can be seen in Figure 3. All the sides of the model are fixed in the x & y directions, and the bottom is fixed in the z-direction that is the vertical direction.

### Viscoelasticity Material Properties

The only material properties that was varied throughout this model were in the P-401 layer (asphalt concrete); the other layer material properties remained constant, which are listed below in Table 5.

Table 5.

Material Properties Used in the Other Layers of the Viscoelasticity Model.

Material	Young's Modulus, ksf (MN/m <sup>2</sup> )	Friction Angle	Dilation Angle	Cohesion, ksf (kN/m <sup>2</sup> )	Density, kslug/ft <sup>3</sup> (kg/m <sup>3</sup> )	Poisson's Ratio
P-209	5760 (275.9)	50	5	0.72 (34.5)	0.005 (2580)	0.3
P-154	2880 (137.9)	45	5	0.922 (44.1)	0.0047 (2420)	0.35
Dupont Medium	1542 (73.8)	0.01	0.0067	2.52 (121)	0.0029 (1520)	0.45

The loading of the model has a single wheel load directly in the center of the top surface. The load follows the same pattern as the FAA Static punch test described previously, which can be seen in Figure 4. The loading for this model is time dependent because it is gradually increased from zero to 55 kips (244 kN) over a period of 50 seconds, and then remains constant for another 200 seconds. This loading allows the viscoelasticity material property to be tested.

## Viscoelasticity Model Results

After the program was run, the deflection was measured under the center of the tire footprint and was compared to the full-scale testing data. From here, the instantaneous elastic modulus could be altered as well as the shift factor for the relaxation times.

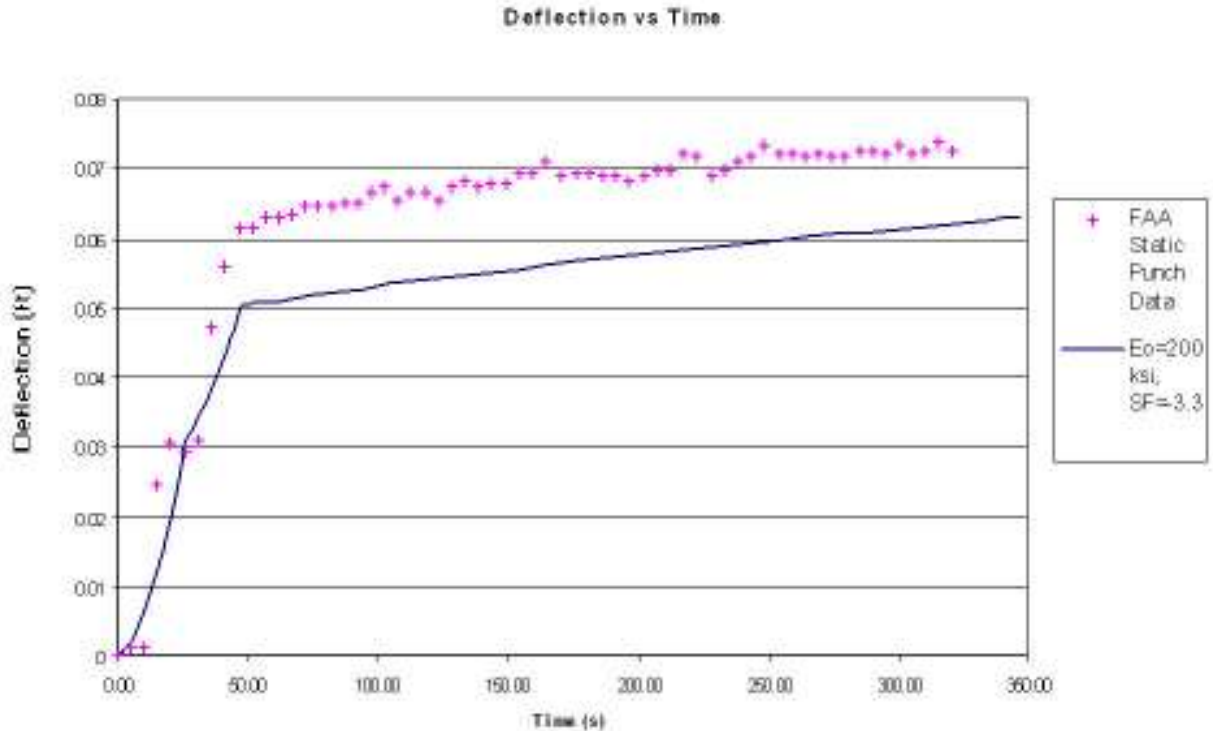


Figure 4. Deflection vs. Time under wheel loading compared to FAA data

When interpreting this graph, it can be seen that the material is acting too stiff to match the FAA data. However, when the elastic modulus value is lowered, the shift factor needs to be altered as well. This model was run constantly changing the elastic modulus and shift factor until the results almost matched perfectly to that of the FAA data. The results of this verification study can be seen in the next section.

## Viscoelasticity Model Conclusions

The final material properties for viscoelasticity of P-401 used in later models are shown in Table 6.

Table 6.  
Prony Series Parameters for P-401 Asphalt Concrete.

Spring Constants, ksi ( $\text{N/m}^2 \times 10^6$ )				
$E_1$	$E_2$	$E_3$	$E_4$	$E_5$
3173 (151.9)	856 (40.9)	2976 (142.5)	3215 (153.9)	3805 (182.2)
Relaxation Times, sec				
$\lambda_1$	$\lambda_2$	$\lambda_3$	$\lambda_4$	$\lambda_5$
0.00643	0.08023	0.65612	5.2108	139.87

The final results for this section are only one of the infinite possibilities that would satisfy the test data. This data is only valid for the temperature of asphalt and the moisture content of the subbase and subgrade, and several other factors at the time of testing.

### Drucker-Prager Material Properties Testing for P-401

The model for Drucker-Prager testing is identical to the one for viscoelasticity; the baseline material properties were established at 500 ksi (3447 MN/m<sup>2</sup>) for elastic modulus, friction angle of 20 degrees, dilation angle of 13.3 degrees, and cohesion of 80 psi (551 kN/m<sup>2</sup>). The subsequent variations changed only one property at a time to determine the effects of altering each one. Table 7 shows the properties for each test.

Table 7.  
Material Properties Tested.

Test	Elastic Modulus, ksf (MN/m <sup>2</sup> )	Friction Angle	Dilation Angle	Cohesion, ksf (kN/m <sup>2</sup> )
DPtest1	72000 (3447)	20	13.3	11.52 (551)
DPtest2	108000 (5171)	20	13.3	11.52 (551)
DPtest3	72000 (3447)	20	13.3	7.2 (334)
DPtest4	72000 (3447)	20	5.0	11.52 (551)
DPtest5	72000 (3447)	30	13.3	11.52 (551)
DPtest6	72000 (3447)	20	5.0	3.6 (172)
DPtest7	72000 (3447)	20	5.0	5.04 (241)
DPtest8	72000 (3447)	20	5.0	4.32 (207)

Once run, the deflection versus loading was compared to the FAA Static punch test. The results are shown in Figure 5, where the load vs. deflection is plotted instead of deflection versus time because the plasticity model is not time dependent only pressure dependent. The graph below shows the results from each model incorporating viscoelastic material properties.

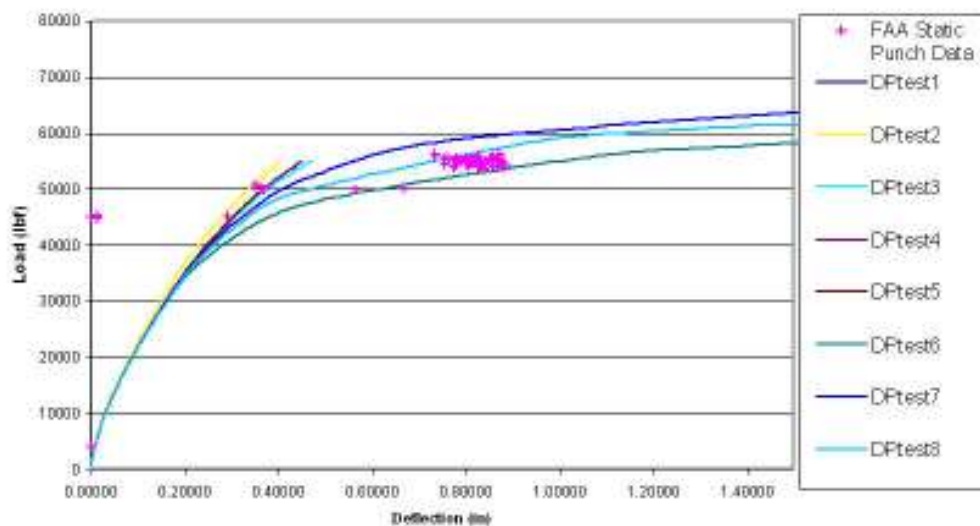


Figure 5. Load vs. Deflection for Drucker-Prager Testing.

The data collected from the output files is compared against the FAA data. The way in which the final material properties were selected was to see which predicted curve intersected with the most real data. The curves for DPtest6 and DPtest7 only encapsulated the data points so a cohesion value between these two curves was chosen. DPtest8 shows that the predicted curve does intersect with some of the FAA data. That is why DPtest8 was chosen to represent the asphalt layer material properties. In the next section the final plasticity material properties can be seen for all the layers.

### Drucker-Prager Model Conclusions

The final material properties of the Drucker-Prager testing for all the layers that are used in the main study are listed in Table 8.

Table 8.  
Final Drucker-Prager Material Properties.

Material	Young's Modulus, ksf (MN/m <sup>2</sup> )	Friction Angle	Dilation Angle	Cohesion, ksf (kN/m <sup>2</sup> )	Density, kslug/ft <sup>3</sup> (kg/m <sup>3</sup> )	Poisson's Ratio
P-401 – Drucker-Prager	72000 (3447)	20	5	4.32 (206)	0.005 (2580)	0.3
P-209	5760 (275.9)	50	5	0.72 (34.5)	0.005 (2580)	0.3
P-154 Dupont Medium	2880 (137.9) 1542 (73.8)	45 0.01	5 0.0067	0.922 (44.1) 2.52 (121)	0.0047 (2420) 0.0029 (1520)	0.35 0.45
Dupont Low	432 (20.7)	0.01	0.0067	4.608 (220)	0.0029 (1520)	0.45

## EFFECT OF WANDER AND GEAR CONFIGURATION ON PERFORMANCE OF FLEXIBLE PAVEMENT SYSTEMS

The main purpose of this paper is to determine the effects of wander and wheel configuration on conventional base, flexible pavement. To do this, material properties were tested to see which match actual data. These properties are then used in two different studies; the first study is loading of one, four, and six wheels on both LFC and MFC pavements to test the effects of wheel configuration and the second study is to determine the effects of wander by testing one wheel with and without wander. Only one wheel is used because the wheel configuration effects could interfere with the results. Due to the limitations of computing power available presently, Drucker-Prager material properties for the asphalt concrete layer (P-401) are used for the study of the effect of wander.

### Study of the Effects of Wheel Configuration

One, four and six wheels are loaded onto both low and medium strength pavement with viscoelastic properties for the asphalt layer. The loading mimics that of the static punch test, instead of 55 kip loading, it is increased to 100 kip, which is ramped over a period of 100 seconds. After the program had run, deflection on the top of the pavement and the vertical stress at the top of the subgrade layer were taken along the line of the loading.

## Wheel Configuration Model Results for LFC Pavement

Figures 6-8 show the results of these models comparing the one, four and six wheels together.

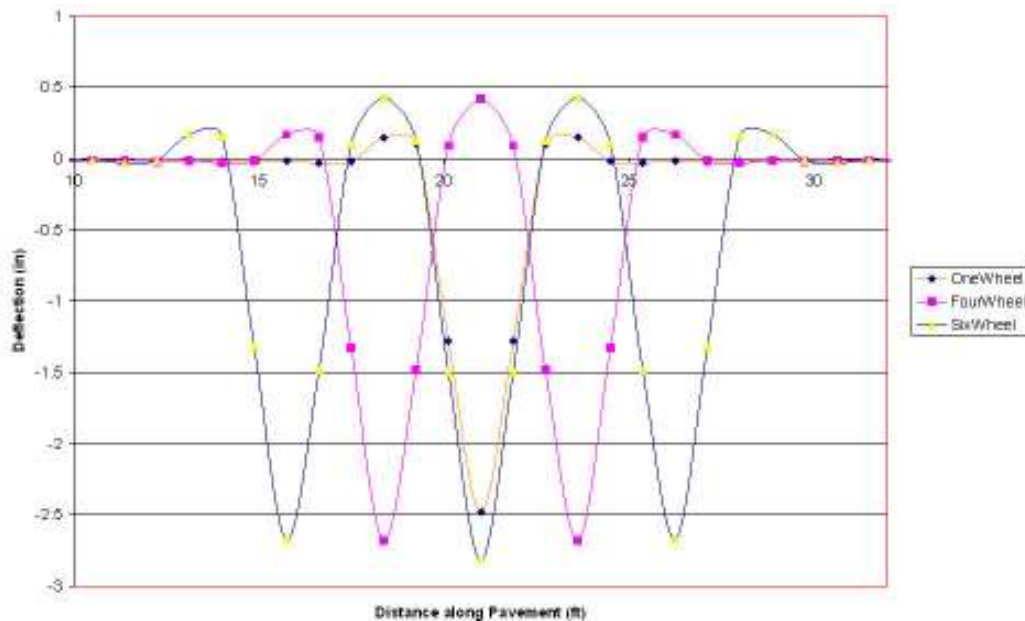


Figure 6. Deflection of Top Surface of LFC Pavement Under 100-kip Loading.

From analyzing Figure 6 above, several observations can be made. First, one wheel upheaval is slightly lower than four and six wheels. Also, one wheel has a smaller maximum deflection as compared to the other two gear configurations. When comparing four and six wheels together, the upheaval is almost identical both on the outside of the wheels and in between the wheels.

## Wheel Configuration Model Results for MFC Pavement

Figures 7 and 8 showing deflections and vertical stresses on the MFC pavement are interesting. It seems as though wheel configuration does not make a significant difference. In the vertical deflection graph above, the upheaval on the outside of each wheel as well as the upheaval between wheels is almost identical.

## Wheel Configuration Model Conclusions

From the results of this section, it can be concluded that on MFC pavement if only vertical stress and deflection are analyzed, gear configuration does not affect the pavement differently. In the LFC pavement, wheel configuration does cause variations in vertical stress and deflection.

## Wander Model

The next study investigates the effects of wander on flexible pavement structure. For this study the landing gear is reduced to only a single wheel. This ensures that wheel configuration does not have an effect on the pavement. Figure 9 shows the abbreviated wander pattern that was used for this simulation.

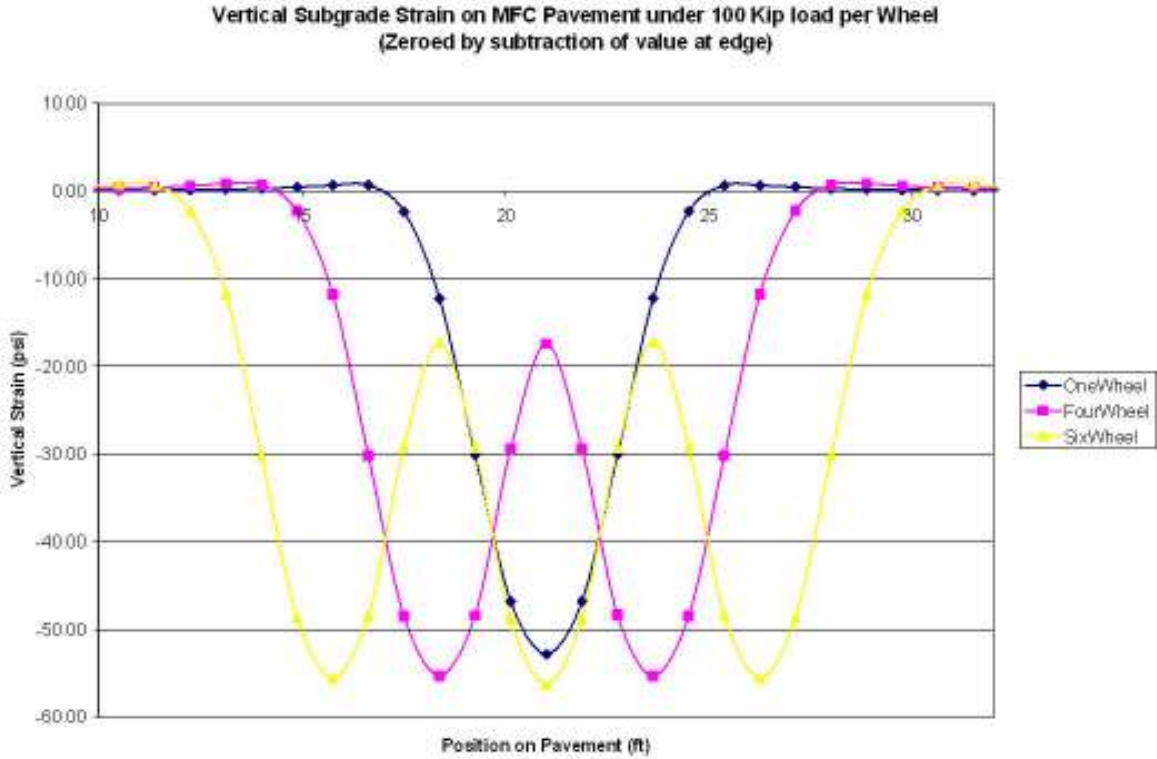


Figure 7. Deflection of Top Surface of MFC Pavement Under 100-kip Loading.

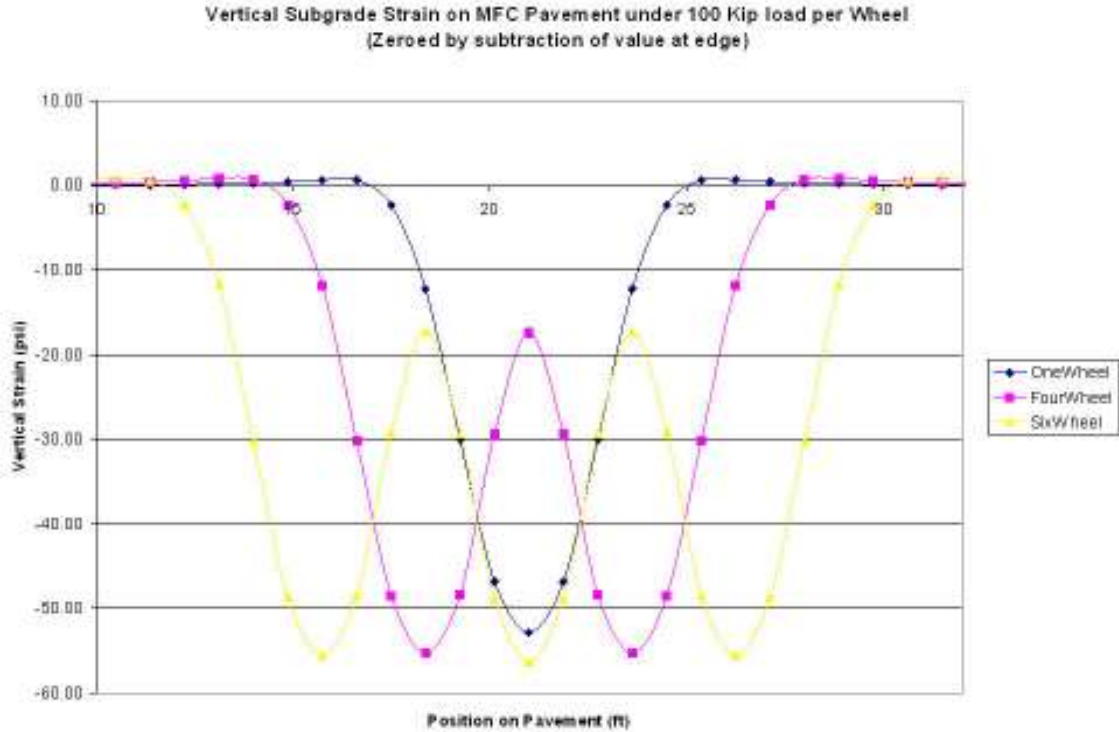


Figure 8. Vertical Stress of Top of Subgrade of MFC Pavement Under 100-kip Loading.

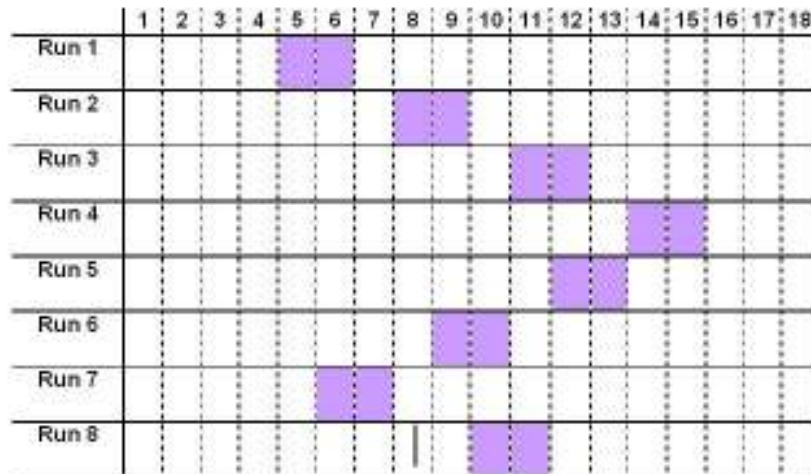


Figure 9. Abbreviated Wander Pattern for Single Wheel.

This mimics the standard distribution that the FAA uses in testing, however instead of 66 runs back and forth, this model only uses 8 runs due to time and memory constraints.

This study compares a single wheel with and without wander to see the effects on the pavement. The wheel has a load of 55 kips on a standard wheel footprint of 12 inches by 21 inches. The overall dimensions of the model are 30 feet by 40 feet by 6 feet deep. The pavement cross section is described as LFC2 pavement, which has a subbase thickness of 24 inches.

### Wander Model Results

Figure 10 compares the vertical deflection in the asphalt layer between one wheel with and without wander. The one wheel without wander causes a larger upheaval deflection of approximately 0.04 inches compared to one wheel with wander that is at 0.025 inches. The upheaval also appears larger than that of one wheel with wander.

Figure 11 shows the plastic strain in the subgrade layer under one wheel with and without wander. One wheel with wander imparts a greater amount of permanent strain over a wider area to the subgrade than a single wheel without wander.

Figure 12 shows the vertical stress at the top of the subgrade layer. These results are taken after all eight runs are completed. On the legend, run 8 is the data for a single wheel without wander and run 8W is for a single wheel with wander. From these results, there is no clear difference in the stresses on the subgrade with and without wander from a single wheel. The single wheel without wander does impart stress on less of an area in the subgrade.

### Wander Model Conclusions

The effects of a single wheel with wander can be seen the most when studying the deflection of the asphalt layer, which shows more deformation under a single wheel without deflection. When analyzing the vertical stress in the subgrade however, there is no clear advantage to

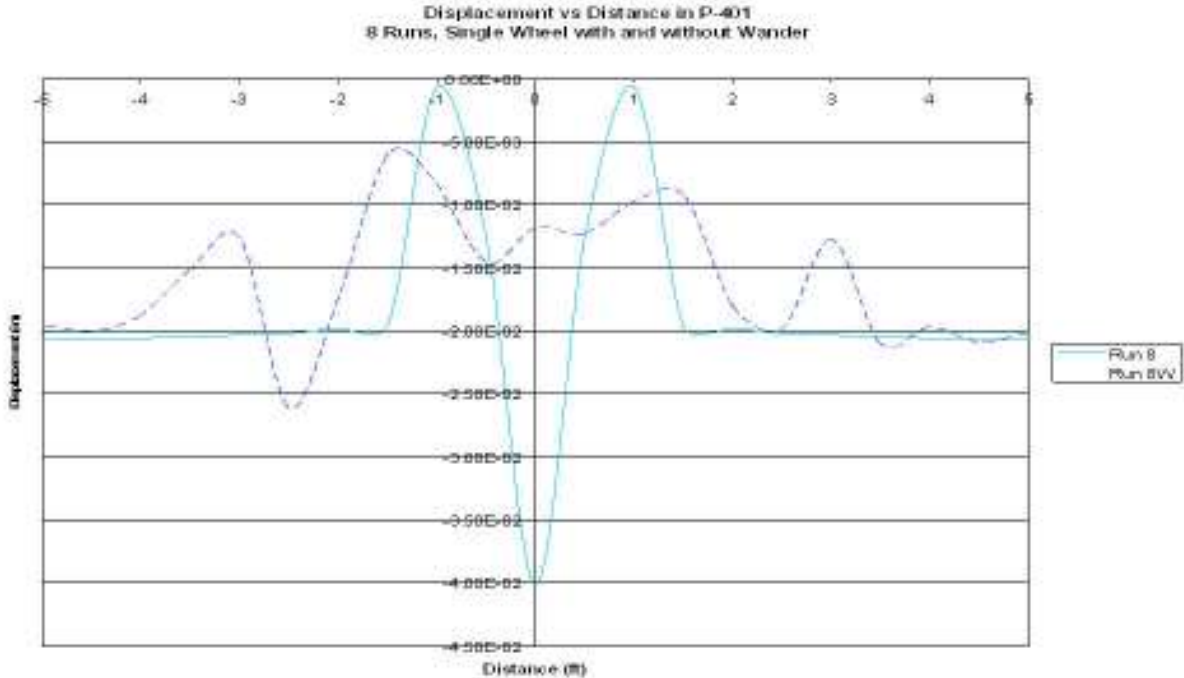


Figure 10. One Wheel With and Without Wander: Vertical Deflection in Asphalt Layer After 8 Cycles.

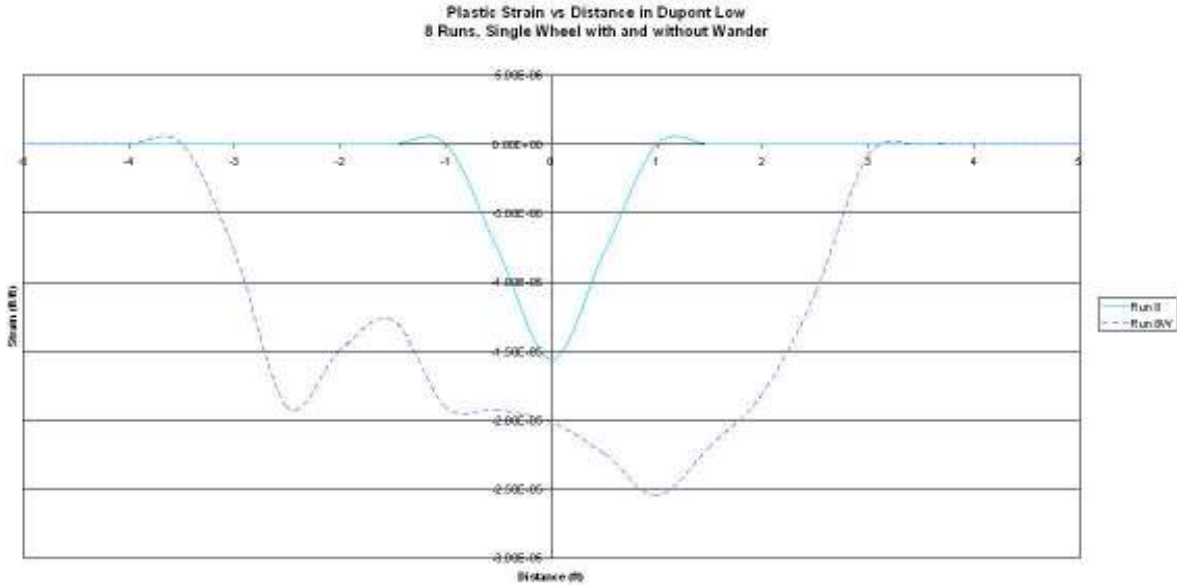


Figure 11. One Wheel With and Without Wander: Plastic Strain in Subgrade Layer After 8 Cycles

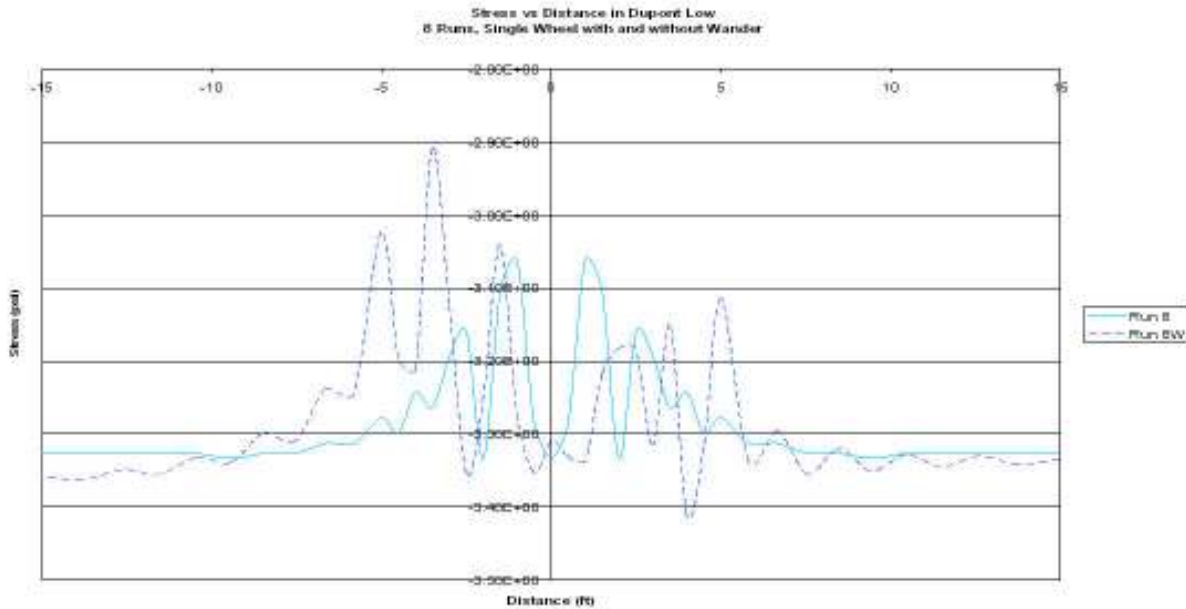


Figure 12. Vertical Stress in Subgrade With Wander and No Wander.

wander. One wheel with wander imparts a greater amount of permanent strain over a wider area to the subgrade than a single wheel without wander.

### Study of the Effects of Wheel Configuration under Quasi-Static Loading

This study compares the effects of a single wheel and a four wheel landing gear on flexible airport pavement. The four wheel landing gear used is modeled after a B747 landing gear. After eight runs back and forth across the pavement surface, the stress, deflection, and elastic and plastic strains are retrieved from each layer. Below some of the results from these simulations can be seen.

Figure 13 compares the deflection in the asphalt layer between one wheel and four wheels without wander. As expected the deflection is greater with four wheels than with one. The maximum deflection with one wheel is only -.02 inches but four wheels is almost twice that at -.04 inches. The upheaval reaches approximately .03 inches with four wheels and only .02 inches with one wheel.

Figure 14 is the vertical stress within the subgrade layer. In this graph, run 8 represents a single wheel and run 8F represents four wheels both without wander. The results show that four wheel gear configuration produces more vertical stress in the layer than a single wheel. It also shows that the area of influence is greater than a single wheel.

### Wheel Configuration under Quasi-Static Loading Conclusions

When comparing one wheel versus four wheels without wander, four wheels cause more deflection in the top layer and more stress to transfer to the subgrade material. It also imparts stress to a greater area than that of a single wheel.

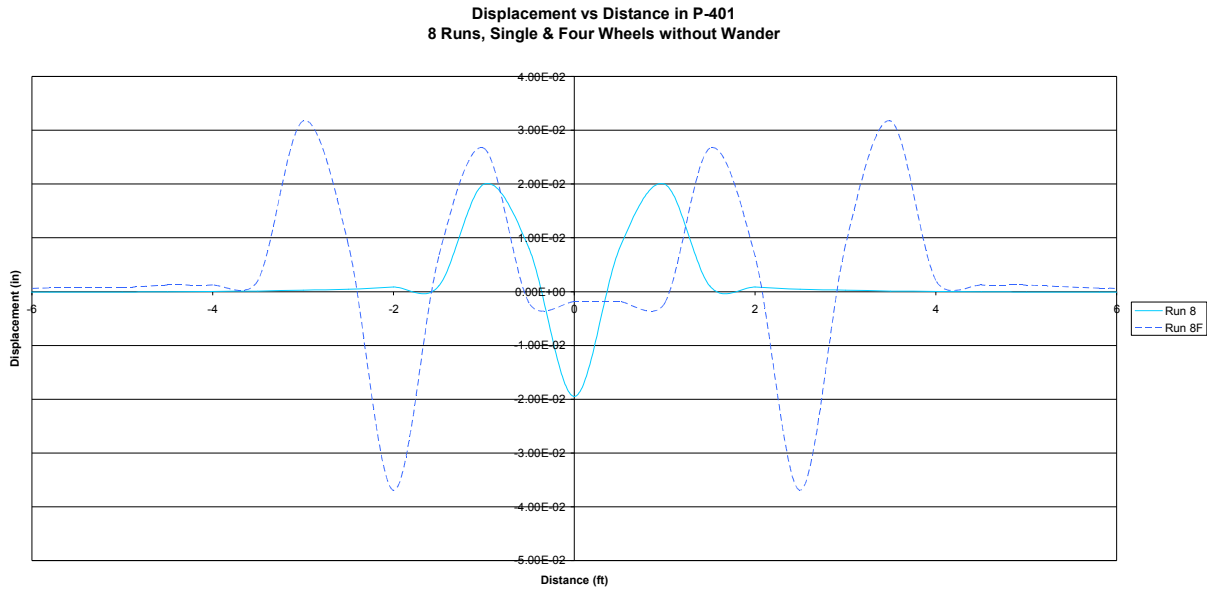


Figure 13. One vs. Four Wheels without Wander: Deflection in Asphalt Layer after 8 Cycles.

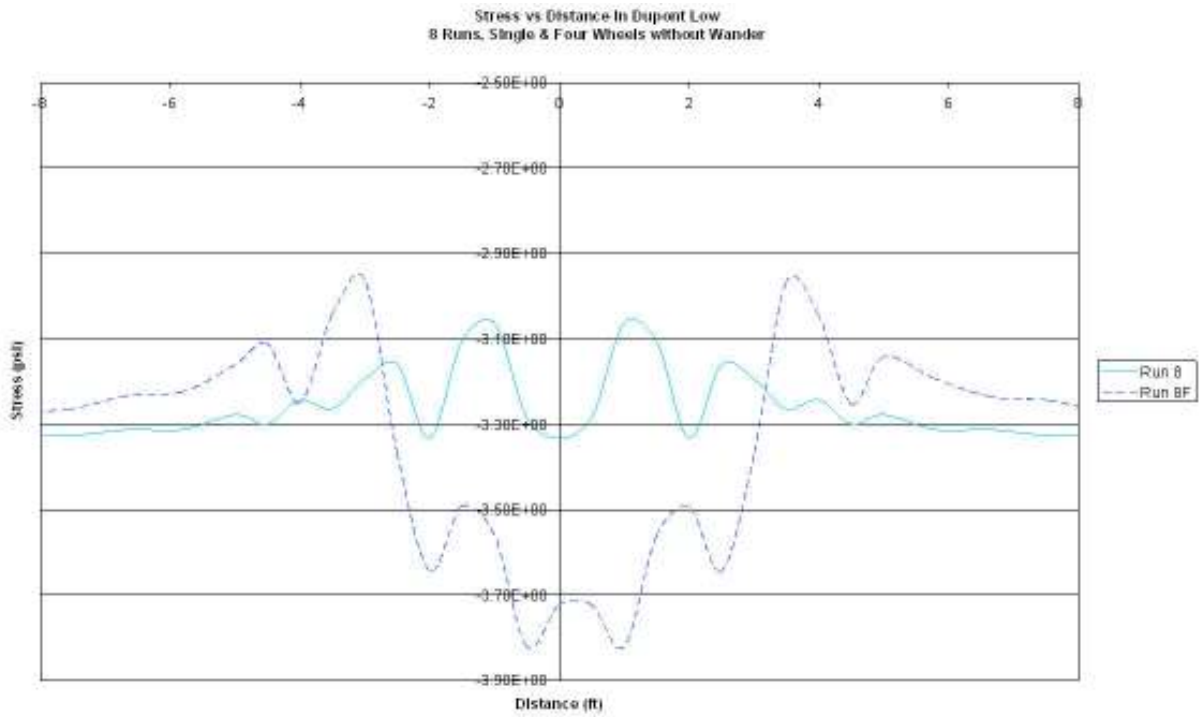


Figure 14. Vertical Stress in Subgrade: One Wheel vs. Four Wheels without Wander.

## CONCLUSIONS

The material properties presented in this paper fit the FAA data well. The option of using viscoelasticity depicts how asphalt would act; however due to memory constraints, it could not

be used in quasi-static or dynamic modeling. Wheel configuration does not effect the pavement differently, when testing MFC pavement. In the LFC pavement, wheel configuration does cause variations in vertical stress and deflection. On LFC2 pavement, four wheel gear configuration causes significant difference in deflection in the asphalt layer and more vertical stress in the subgrade layer. The advantage to single wheel wander can be seen when analyzing the deflection in the asphalt layer, which showed significant difference between wander and no wander. The vertical stress in the subgrade for wander showed no major difference between the two. One wheel with wander imparts a greater amount of permanent strain over a wider area to the subgrade than a single wheel without wander.

## ACKNOWLEDGMENTS

This research work is supported by award 2005G-016 from the Federal Aviation Administration, which is gratefully acknowledged. The help provided by Dr. Gordon Hayhoe, Dr. David Brill and staff at the NAPTF for this research is also gratefully acknowledged.

## REFERENCES

1. National Airport Pavement Facility, <http://www.airporttech.tc.faa.gov/naptf/>.
2. Chen, D. H., Zaman, M., Laguros, J., Soltani, A., "Assessment of computer programs for analysis of flexible pavement structure," Transportation Research Record 1482, TRB, National Research Council, Washington, D., C., 1995, 123-133.
3. Cho, Y-H., McCullough, B.F., and Weissman, J., "Considerations on finite element method application in pavement structural analysis," Transportation Research Record 1539, TRB, National Research Council, Washington, D., C., 1996, 96-101.
4. Kuo, C. M., K. T., and Darter, M. I., "Three dimensional finite element model for analysis of concrete pavement support, Transportation Research Record 1505, TRB, National Research Council, Washington, D., C., 1995, 119-127.
5. Nazarian, S. and K. M. Boddspati, "Pavement-Falling Weight Deflection Interaction Using Dynamic Finite Element Analysis," Transportation Research Record 1449, TRB, National Research Council, Washington, D., C., 1995, 123-133.
6. Zaghoul, S.M., and T.D., White, "Use of a Three-Dimensional, Dynamic Finite Element Program for Analysis of Flexible Pavement," Transportation Research Record 1388, TRB, National Research Council, Washington, D., C., 1993, 60-69.
7. HKS, ABAQUS Theory and Users Manual – Version 6.3, Hibbit, Karlsson & Sorenson, Inc., Pawtucket, Rhode Island., 2006.
8. Sukumaran, B., Kyatham, V., Shah, A., Sheth, D., "Suitability of Using California Bearing Ratio Test to Predict Resilient Modulus," Airport Technology Transfer Conference, Atlantic City, NJ, May, 2002.
9. Willis, Michael, Three dimensional finite element analysis as a tool for flexible pavement design and analysis, Master's thesis, 2005, Rowan University.
10. Bozkurt, D., and W. G. Buttlar, "Three-Dimensional Finite Element Modeling to Evaluate Benefits of Interlayer Stress Absorbing Composite for Reflective Crack Mitigation," Airport Technology Transfer Conference, Atlantic City, NJ, May, 2002.